Modeling a Well-Characterized Perfluorooctane Sulfonate (PFOS) Source and Plume Using the REMChlor-MD Model to Account for Matrix Diffusion

Poonam R. Kulkarni[1], David T. Adamson[2], Jovan Popovic[3], Charles J. Newell[2]

[1] Corresponding author: prk@gsi-net.com; GSI Environmental Inc., Houston, Texas, United States

[2] GSI Environmental Inc., Houston, Texas, United States. dtadamson@gsi-net.com, cjnewell@gsi-net.com.

[3] Naval Facilities Engineering and Expeditionary Warfare Center, Port Hueneme, CA, 93041 USA. jovan.popovic@navy.mil

KEYWORDS

PFAS, PFOS, Matrix Diffusion, Fate and Transport, Modeling, REMChlor-MD, Remediation

ABSTRACT

Two of the most important retention processes for per- and polyfluoroalkyl substances (PFAS) in groundwater likely are sorption and matrix diffusion. The objective of this study was to model concentration and mass discharge of one PFAS, perfluorooctane sulfonate (PFOS), with matrix diffusion processes incorporated using data from a highly chemically- and geologically-characterized site. When matrix diffusion is incorporated into the REMChlor-MD model for PFOS

at this research site, it easily reproduces the field data for three key metrics (concentration, mass discharge, and total mass). However, the no-matrix diffusion model produced a much poorer match. Additionally, after about 40 years of groundwater transport, field data and the REMChlor-MD model both showed the majority (80%) of the measured PFOS mass that exited the source zones was located in downgradient low permeability zones due to matrix diffusion. As such, most of the PFOS mass is not available to immediately migrate downgradient via advection in the more permeable sands at this site, which has important implications for monitored natural attenuation (MNA). Plume expansion over the next 50 years is forecasted to be limited, from a 350-meter plume length in 2017 to 550 meters in 2070, as matrix diffusion will attenuate groundwater plumes by slowing their expansion. This phenomenon is important for constituents that do not degrade, such as PFOS, compared to those susceptible to degradation. Overall, this work shows that matrix diffusion is a relevant process in environmental PFAS persistence and slows the rate of plume expansion over time.

INTRODUCTION

PFAS have recently appeared as a chemical of emerging concern in soil and groundwater. Several quantitative metrics indicate the potential scale of future cleanup of groundwater sites with PFAS could be extensive (Newell et al., 2020). Specifically, a symposium of 60 PFAS experts concluded that due to their mobility, persistence, and technical limitations to remediation, PFAS present more complex challenges as compared to other chemicals (Simon et al., 2019). While Simon et al., (2019) noted there are some uncertainties regarding PFAS transport parameters,

conservatives assumptions can be used to evaluate different scenarios for PFAS transport.

Developing appropriate fate and transport modeling approaches for PFAS is critical for evaluating risk at impacted sites, as well as understanding what remedies or site management options are viable for addressing that risk. Without the ability to make planning-level predictions about plume behavior over time, it is difficult for decision-makers to avoid expensive cleanup technologies such as groundwater pump and treat as a conservative measure. It also limits the technical justification for selecting less-intensive strategies for PFAS such as Monitored Natural Attenuation (MNA). MNA already faces a significant hurdle in that PFAS are not expected to transform beyond perfluoroalkyl acids (PFAAs) under natural environmental conditions. However, retention-based processes can form the basis for applying Monitored Natural Attenuation to manage PFAS impacts in groundwater (Newell et al., 2021a, Newell et al. 2021b), assuming an understanding of how these processes influence PFAS plumes can be established.

Two of the most important retention processes for PFAS in groundwater are likely to be sorption and matrix diffusion. The extent to which sorption contributes to retardation of PFAS during groundwater transport is a function of aquifer properties but also the complex and diverse physical-chemical properties of PFAS as a chemical class (Higgins et al., 2007, Anderson et al., 2019, Adamson et al., 2021). Because they exhibit surfactant-like properties, PFAS can partition to air/water interfaces that are present within the pore space in the unsaturated zone. PFAS can sorb hydrophobically to naturally occurring organic matter on soils, to Non-Aqueous

73 Phase Liquids (NAPLs), and through electrostatic interactions with soil mineral
74 phases. Because PFAS are typically released to the environment as a mixture with
75 various different charges (some are anions, some cations, some zwitterions) and
76 hydrophobicity, individual PFAS can have a range of sorption characteristics. For
77 example, long chained PFAS will usually sorb more readily than short chained
78 PFAS, and desorption hysteresis and competitive sorption among different PFAS
79 have the potential to impact PFAS transport (Sima and Jaffe, 2021). Similarly,
80 cationic and zwitterionic PFAS will tend to sorb more readily to soils than anionic
81 PFAS such as PFOS and PFOA (Guelfo et al., 2013, Li et al., 2018) given the
82 negative surface charges associated with many soil particles (e.g., clays).

83

84 The role of matrix diffusion in groundwater transport was first identified by Foster
85 (1975) in the Chalk aquifer in southern and eastern England. This term is used to
86 describe the concentration gradient-driven mechanism where chemicals are
87 exchanged from media with high permeability to regions of lower permeability (or
88 “low-k”, as described in Sale et al. [2013]) diffusion. Sudicky et al., (1982) and
89 Gillham et al. (1984) initially showed how matrix diffusion can slow and attenuate
90 solutes moving in heterogeneous geologic settings.

91

92 Another key consequence of matrix diffusion is the chemical release from low-k
93 zones via back diffusion (outward diffusion) and slow advection once the
94 concentrations in the transmissive zones drop either due to natural or engineered
95 reduction in source strength or direct remediation of groundwater plumes (Chapman
96 and Parker, 2005; NRC, 2005; Sale et al., 2008; NRC, 2013; Sale et al., 2013;
97 USEPA, 2019; You et al., 2020; Brooks et al., 2021).

Factors controlling the rate of diffusion to and from low-k regions include diffusion and slow advection. Diffusion incorporates the difference in concentrations between the transmissive and low-k media, the amount of time chemicals are in contact with low-k zones, the diffusivity of the chemicals, and the porosity/tortuosity of the low-k media (Sale et al., 2013). Modeling matrix diffusion can prove challenging because there are only limited number of commercially available analytical groundwater models that account for matrix diffusion (e.g., Chapman et al., 2012; Farhat et al., 2012; Muskus and Falta, 2018; Falta et al., 2018) and numerical models can result in erroneous results if the vertical discretization is too coarse (Chapman and Parker, 2005; Farhat et al., 2020). However, failing to account for matrix diffusion in models leads to faulty predictions, thus hindering effective remediation strategies (Adamson and Newell, 2014; OSWER, 2019).

There has been extensive research on trying to model PFAS transport in the vadose zone (e.g., Brusseau, 2018; Brusseau et al., 2019; Constanza et al., 2019; Silva et al., 2020; Guo et al., 2020). However, there are very few reports of groundwater modeling of PFAS fate and transport in the saturated zone, particularly those that evaluate plume behavior over time. In a recent study by Farhat et al. (2021), the REMChlor-MD model (Falta et al., 2018) was applied to explore the general behavior of non-degrading groundwater plumes like PFOS and PFOA, particularly with regard to retention-based attenuation caused by matrix diffusion processes. The resulting analysis concluded that non-degrading plumes would continue to expand over time assuming a constant source, but matrix diffusion will result in lower concentrations and smaller footprints. For instance, in a 100-year

travel time scenario modelled with matrix diffusion, the resulting PFOS plume length was only 20% as long as a scenario without matrix diffusion (Farhat et al., 2021). These results help highlight the potential relevance of matrix diffusion on PFAS fate and transport, which along with sorption and partial biotransformation could be expected to influence PFAS retention within heterogeneous saturated zones.

This study presents a novel application of a matrix diffusion model (REMChlor-MD) to simulate the history and potential future migration of an actual PFOS plume at a well-characterized research site. Here, PFOS transport was modeled using site-specific data from a highly chemically and geologically characterized fire training area (FTA) where significant PFAS mass was encountered in low-k soils (Nickerson et al., 2020; Adamson et al., 2020). Because the current state of knowledge suggests that PFOS does not degrade in the environment, the modeling focuses on non-destructive attenuation processes such as sorption and matrix diffusion. As such, the objective of this study was to model concentration and mass discharge of PFAS with matrix diffusion processes incorporated to show how these influence plume length and remedial performance. This work establishes, as with almost all contaminants, that contaminant storage and release to and from low k zones (matrix diffusion, slow advection) is also relevant in PFAS source zones and plumes. As with many contaminant releases, failing to consider matrix diffusion has the potential to lead to flawed assessments of risk and/or selection of remedies for PFAS releases.

SITE BACKGROUND

The study area is a former firefighting training facility located within a military installation in the United States. A high-resolution site characterization program was conducted in 2017, consisting of 16 locations selected from within the source and downgradient areas. Here, site characterization was conducted in the upper 10-15 m of a surficial aquifer using a Hydraulic Profiling Tool (HPT), as well as collecting co-located depth-discrete soil and groundwater samples using a Geoprobe drilling rig. A detailed description of the field sample collection methods and analytical protocols are provided in Nickerson et al., (2020).

A total of 58 groundwater samples were collected and analyzed for 79 PFAS at Oregon State University (OSU), while 105 soil samples were collected and analyzed for 136 PFAS at Colorado School of Mines (CSM) (Adamson et al., 2020; Nickerson et al., 2020). Both the groundwater and soil data were used to quantify the following PFAS groupings: (1) PFOS; (2) PFOA; (3) Total PFAAs; (4) Total Cations and Zwitterions; (5) Total Precursors; and (6) Total PFAS.

Hydrogeology

Based on results from subsurface drilling using a Hydraulic Profiling Tool (HPT) and logging of cores collected during the field characterization, there are four main soil types in the water-bearing unit. Using the Universal Soil Classification System (USDA, 2012), these were: (1) Poorly Graded Sands (SP); (2) Sands with Fines (SM); (3) Silt (ML); and (4) Clays with low plasticity (CL).

Specifically, the subsurface at this site is composed primarily of permeable sands and less permeable silts and clays (Adamson et al., 2020). Sands dominate the first 1 to 2 meters of the site, forming a thin vadose zone as a shallow aquifer is encountered within the first two meters of the subsurface. Laterally extensive clays appear at depths between 3 to 4.5 meters, with a second layer of silt/clay present at around 10 meters (Nickerson et al., 2020). Additionally, based on site documents describing the hydrologic setting, the aquifer consists of undifferentiated terrace and shallow marine deposits of Pliocene to Holocene age associated with glacial and inter-glacial periods (USGS, 2000). Figure 1 shows a cross section of the study site along the direction of groundwater flow depicting key soil types and stratigraphy. Groundwater flows in a north to northeast direction from the study area towards a river (Nickerson et al., 2020).

Two slug test results were available for two monitoring wells screened in the most transmissive geologic media, Poorly Graded Sands (SP) as defined by the Universal Soil Classification System (USDA, 2012). Here, slug test results together had geomean hydraulic conductivity of 2.4×10^{-3} cm/sec (6.8 ft/day) (Consultant Report, 2017). When combined with an estimated effective porosity of 0.10 and the measured hydraulic gradient of 0.00375 m/m, the estimated seepage velocity for the most transmissive sands was 28 m/year (93 ft/year). The effective porosity is a key parameter for the transport model applied at this site. The environmental consulting company that performed the slug tests used an effective porosity of 0.05 for their seepage velocity calculations, citing "*While silty sand may have an average porosity of between 25 and 60 percent, the effective porosity is usually estimated at about 5 percent."* (Consultant Report, 2017). These effective porosities, while lower

than some groundwater modeling studies, are supported by the “mobile porosity” model developed by Payne et al. (2008) that was based on approximately 15 detailed tracer tests at remediation sites. Similarly, Kulkarni et al. (2020) evaluated 141 boring logs from 43 sites to develop an empirical estimate of a representative mobile porosity, resulting in a value of approximately 0.11.

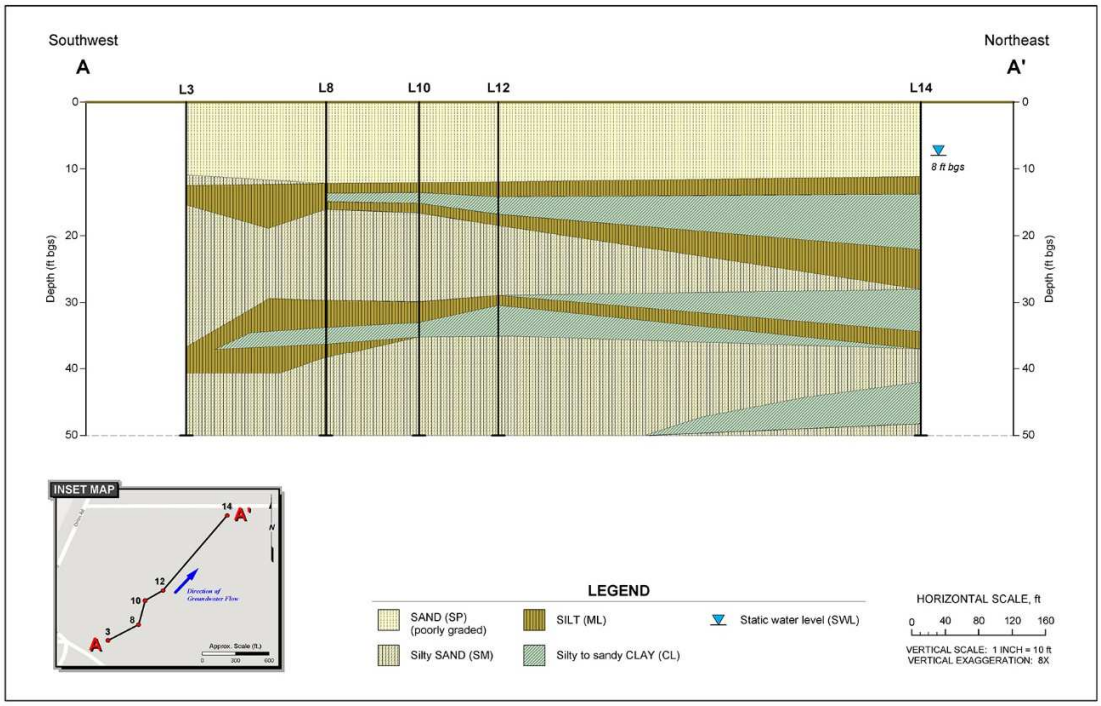

Figure 1. Geologic Cross-Section of Site Along Direction of Groundwater Flow

Additionally, three spatial compartments were used to define the PFAS plume: Source Transect, Near Downgradient Transect, and Far Downgradient Transect. Figures 2 and 3 depict the relative distribution of the different soil types in the three spatial compartments.

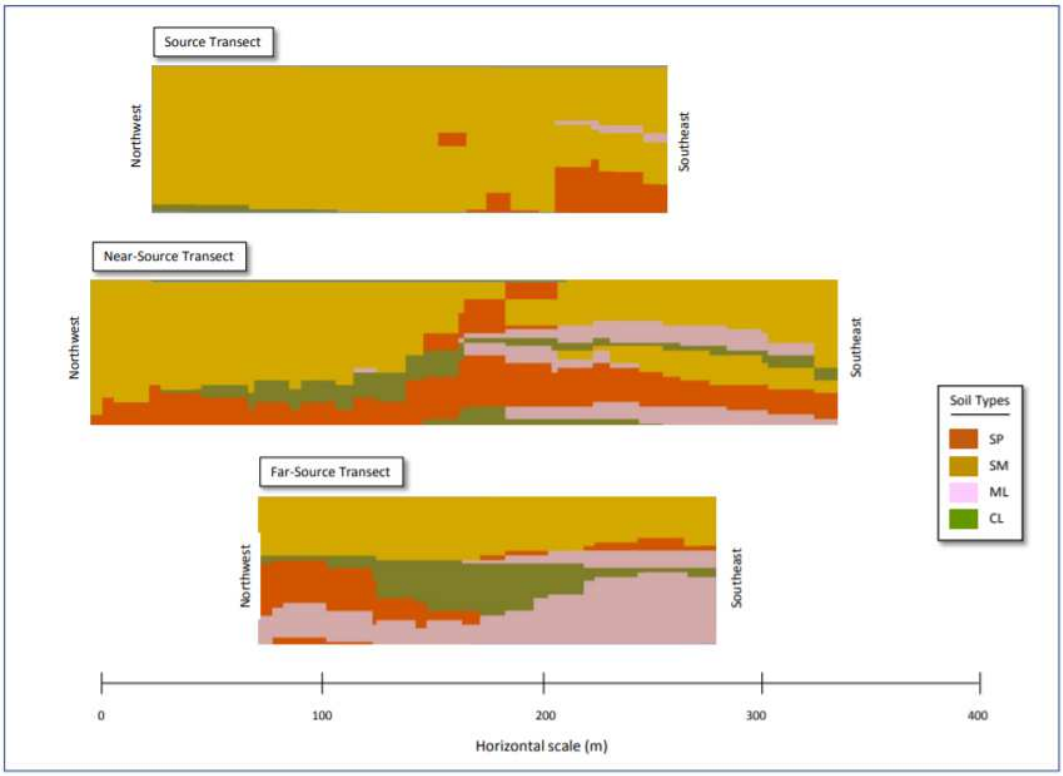

208

209 **Figure 2. Soil Type Across Three Transects (Reprinted with permission from**
210 **Adamson et al., 2020. Copyright 2020 American Chemical Society).**

211

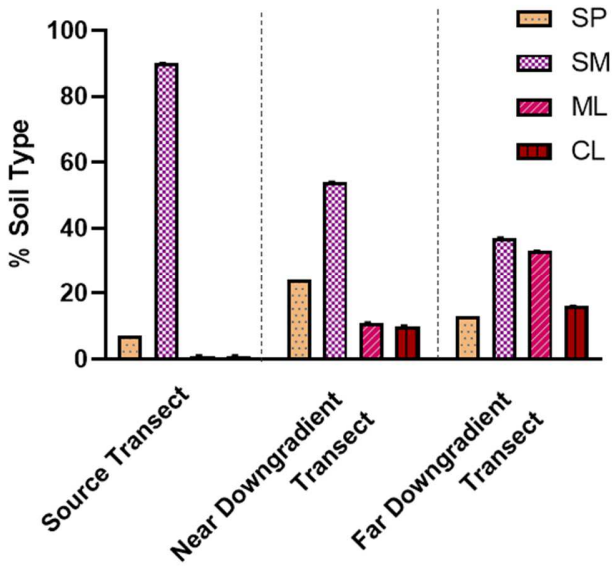

212

213 **Figure 3. Distribution of Soil Types by Transect.** Transect locations and cross-sections
214 depicted in Figure 2

PFAS Source and Plume Characteristics

Between 1968 and 1991, site personnel used aqueous film-forming foam (AFFF) while training to extinguish fires in a pit measuring approximately 36 meters in diameter (Adamson et al., 2020; Nickerson et al., 2020). Given the known presence of PFAS in AFFF, a site characterization was carried out starting in 2017 in an effort to determine the spatial distribution of PFAS in the shallow aquifer (Adamson et al., 2020; Nickerson et al., 2020). While AFFF was only released within the training pit, impacts to adjacent areas is possible due to overspray (Adamson et al., 2020; Nickerson et al., 2020)). Soils from the study area have previously been the focus of a 1994 remediation project for non-PFAS chemicals where petroleum-impacted soils were removed from the pit and remediated at a mobile low-thermal desorption treatment unit (Adamson et al., 2020; Nickerson et al., 2020). Following treatment, the soils were returned to the pit.

Based on depth-discrete groundwater sampling, Figure 4 depicts the PFOS groundwater plume at the site. Figure 5 uses depth-discrete soil sampling data to show a three-dimensional depiction of PFOS mass in subsurface soil.

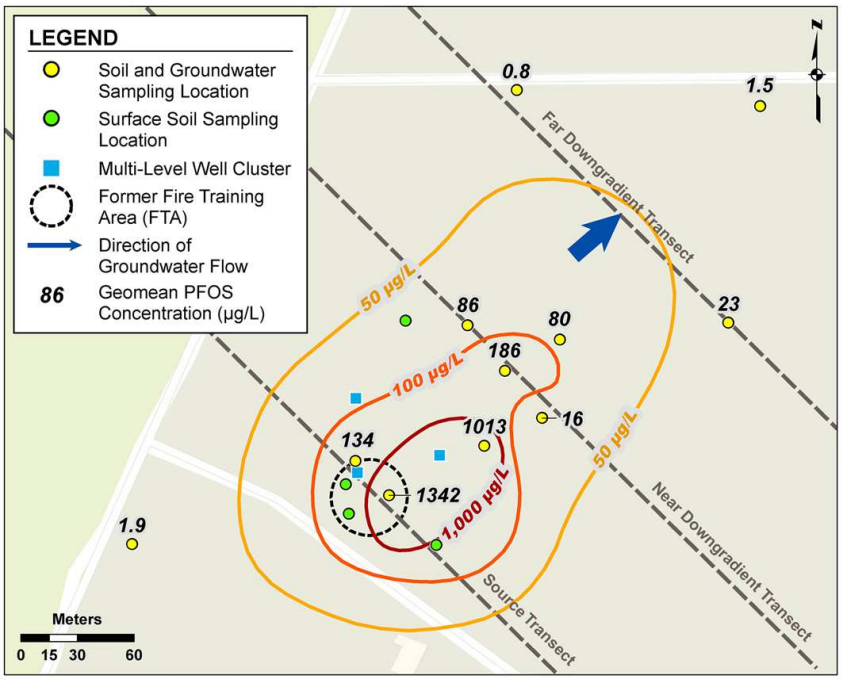

Figure 4. PFOS in Groundwater Plume Map. Concentrations represent geomean of depth-discrete samples at 3.05 m and 6.1 m bgs.

METHODS

PFAS Mass and Mass Discharge Estimation Process

Adamson et al. (2020) employed the Voxler® interpolation tool (Version 4.6.913, Golden Software, 2019) to develop a three-dimensional grid of the PFAS data and soil types. As described by Adamson et al. (2020), a total of 58 groundwater samples were analyzed for 79 PFAS compounds by Dr. Jennifer Fields' lab at Oregon State University (OSU). These data were kriged using GMS and then used by the Voxler tool to develop a three-dimensional model of soil concentrations for key PFAS and PFAS classes and for soil type. The Voxler tool was then able to calculate masses of these categories in different regions of the site (e.g., source, near downgradient, far downgradient) and in different soil types. A total of 105 soil samples were analyzed for 136 PFAS compounds by Dr. Chris Higgins' lab at the

Colorado School of Mines (CSM). The Voxler model was used to construct a three-dimensional model of concentrations for key PFAS and PFAS categories which was then used to calculate mass discharge across the three transects (Adamson et al., 2020). A visualization of the PFOS subsurface mass generated by the Voxler model is shown in Figure 5.

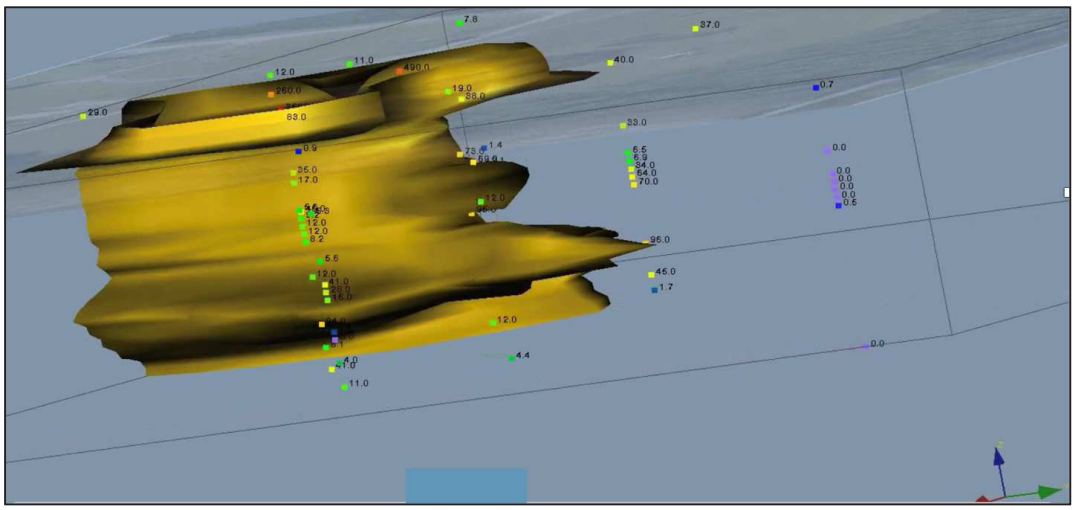

Figure 5. Three-Dimensional Depiction of PFOS Mass in Soil with Cutoff Limit of 100 ng/kg.

Additionally, the PFAS compartment model provided a quantitative dataset showing where PFAS were distributed in the subsurface in 2017, including how much was in the source vs. plume, in the transmissive vs. low-k geologic media, and in the aqueous-phase vs. sorbed phase (see Figures 1, 2, and 3 respectively in Adamson et al., 2020). Here, the source was defined by knowledge of historic site activities and their spatial footprint, as well as site-characterization data confirming significantly higher concentrations. Additionally, the mass discharge data showed the rate that PFAS are transported through the transmissive zone at three different vertical transects of the source/plume system to establish the physio-chemical natural attenuation of PFAS at this site.

For the current modeling study, PFOS was selected as the PFAS of interest because it was the most prevalent PFAS, representing 40 kg of the total 222 kg of Total PFAS at the site (Adamson et al., 2020). Key PFOS mass in various soil types from the Voxler tool are shown in Table 1:

Table 1. PFOS Mass by Spatial Location and Soil Type (kg)

Spatial Location	Total	SP	SM	ML	CL
	Mass (kg)				
Up/Side-Gradient Plume	10.4	1.7	8.1	0.5	0.0
Source	6.6	1.5	4.9	0.3	0.0
Near Downgradient	16.9	2.9	11.4	2.3	0.3
Far Downgradient	6.0	1.8	2.1	0.9	1.3
Total Source + Plume	***39.9***	***7.8***	***26.4***	***4.0***	***1.7***

Note: PFOS mass per soil type depicted in light yellow (0-0.9 kg), dark yellow (1-4.9 kg), and orange (>5 kg).

The tool also yielded three PFOS mass discharge values for the three transects shown in Figure 2:

- Source Transect (0 m from source): 0.31 kg/yr (87% through SP soils)
- Near Downgradient (114 m from source): 0.13 kg/yr (98% through SP soils)
- Far Downgradient (190 m from source): 0.0053 kg/yr (85% through SP soils)

For estimating the source mass discharge history that was applicable at this site, several commonly used options that involve simple functions over time were initially considered (e.g., Newell and Adamson, 2005):

- Constant source over time until the source mass is depleted (Step Function);
- Linearly decaying source until the source mass is depleted; and
- Exponentially decaying source based on the source mass.

A more sophisticated source model that was also considered was the power function model (sometimes referred to as the “gamma model”) where the change in

291 source strength over time is a function of the change of source mass over time to a
292 defined power (gamma) (Rao et al., 2001; Falta et al., 2005). Assigning a value of
293 zero for gamma gives a step function for the source strength, 0.5 gives a linear
294 decline in source strength, and a gamma of 1.0 gives an exponential decay. Other
295 values give a hybrid between these different models, with values greater than 1.0
296 giving long, slowly changing extended source strength tails.

297

298 To determine which of these simple models was best suited for modeling the PFOS
299 source strength over time at this research site, an initial exploratory evaluation of
300 the 2017 mass and mass discharge data was performed. The best available site
301 records indicated that fire-fighting training activities at the site with AFFF started in
302 approximately 1968, although the records are not definitive. In general, PFAS-
303 containing fire-fighting foams for the U.S. military were introduced in the late-1960s
304 (3M, 2021), so much earlier dates of release to groundwater are unlikely. Later
305 releases to groundwater are possible, particularly considering the time it takes for
306 PFAS from the vadose zone source to migrate to groundwater (e.g., Guo et al.,
307 2020). By the year 2017 (49 years later), the mass of Total PFAS in the
308 downgradient plume was measured to be 117 kg, and the mass discharge from the
309 source/upgradient/side gradient zones was estimated to be 3.6 kg/yr (Adamson
310 et al., 2020). While these are not precise estimates due to uncertainties in the
311 historical record and in the mass and mass discharge calculations, they can form
312 the basis for developing a hypothesis regarding the source strength history. For
313 example, a constant mass discharge of 3.6 kg/yr of PFAS over 49 years (1968 to
314 2017) would have delivered 176 kg of PFAS to the downgradient plume, about 1.5
315 times the measured mass. A higher source in 1968 that declines to 3.6 kg/yr in

316 2017 would have introduced even more PFAS mass to the downgradient plume,
317 increasing the discrepancy between modeled and measured PFAS mass. This
318 information suggested the best model for fitting these data was a constant source
319 (step function).

320

321 However, even the constant source model overpredicted the measured
322 downgradient plume PFAS mass in 2017. Therefore, the initiation of PFAS mass
323 discharge to the downgradient plume was hypothesized to start nine years after
324 1968 in 1977 to yield a calculated downgradient mass of 144 kg (3.6 kg/yr x 40
325 years) compared to the measured mass of 120 kg. It is possible that fire-fighting
326 training was started at a low level in 1968, but then increased significantly in the late
327 1970s. The better match with the 40-year time may also be caused by the slow
328 vertical migration of the PFAS through the vadose zone, where it might have
329 partitioned to the air/water interfaces, and then via slow downward radial flow to
330 groundwater. No degradation of Total PFAS was assumed because any
331 transformation of PFAS precursors would have been matched by a similar mass of
332 PFAA's generated from the transformation.

333

334 The matches for individual PFAS varied. The constant source model overestimated
335 PFOS mass in the downgradient plume by 44% but underestimated PFOA by about
336 50%). The match between constant source model and the measured field data were
337 relatively close for PFAAs and Total Precursors (data not shown). Because of this
338 variability between different PFAS and PFAS classes, the timing analysis based on
339 the Total PFAS mass discharge and measured downgradient Total PFAS mass was
340 used for the modeling analysis. Overall, this comparison concludes that unlike the

mass discharge patterns typically observed at chlorinated solvent or benzene, toluene, ethylbenzene, xylene (BTEX) sites (e.g., see Newell et al., 2014), this PFAS site may have had a relatively constant mass discharge from the source for the past ~40 years.

Because PFOS was the key focus of this modeling research, an additional evaluation was performed to increase the confidence in these field-based mass estimates. An independent analysis of the potential amount of PFOS that could have been introduced into the subsurface was performed based on historical use data at firefighting training sites, as described in Adamson et al., (2020), Supplemental Information. This historical usage estimate indicated it was possible that about 81 kg of PFOS could have been released during fire-fighting training events during the lifetime of the site. The 81 kg is within a factor of two compared to the more reliable measured PFOS mass of 40 kg, a relatively close match considering the uncertainties in the historic usage estimate. Additional uncertainties include the transformation of precursors to PFOS (historically or ongoing), as no precursors or biotic transformation to PFOS has been accounted for in mass estimates in the source or downgradient because rate data are relatively limited (Adamson et al., 2020). In addition, the site data presented in Adamson et al. (2020) showed that precursors were primarily located in the source area, such that transformation to PFOS within the plume would be minimal.

365 **REMChlor-MD Model Overview**

366 These data were used to evaluate a novel application of a recently released ESTCP
367 groundwater fate and transport model, REMChlor-MD (Falta et al., 2018; Farhat et
368 al., 2018), for the PFOS plume at the site. While designed for chlorinated solvent
369 sites, REMChlor-MD can be adapted to simulate groundwater transport at PFAS
370 sites. REMChlor-MD consists of a simple source model coupled to a semi-
371 analytical plume transport model. The source model uses a power-law relationship
372 to define the long-term relationship between the remaining source mass and the
373 mass discharge leaving the source at any time. The plume model uses a semi-
374 analytical method with defined gridblocks to simulate advection, dispersion,
375 retardation, and degradation. In addition, the plume model can simulate matrix
376 diffusion effects for two different geologic configurations: 1) low-k aquitards in
377 contact with transmissive geologic media, and 2) the effect of low-k layers and
378 lenses embedded within the transmissive media. The embedded matrix diffusion
379 term was derived by Falta and Wang (2017) and Muskus and Falta (2018) by
380 adapting heat conduction models developed by Vinsome and Westerveld (1980).
381 To use this feature in the model, users enter transmissive vs. low-k layering
382 information contained in existing geologic boring logs into the model's
383 "heterogeneity calculator" which then calculates three key matrix diffusion variables
384 used by the model: 1) the volume fraction of low-permeability material; 2) the
385 characteristic maximum matrix diffusion length; and 3) the surface area of the
386 transmissive/low-k interfaces within each defined gridblock.

387

388 With the high-resolution field data, reliable estimates of the mass of different PFAS
389 and PFAS groups were used to bound how much PFAS was released at the AFFF

390 Fire Training Facility and the original mass discharge to groundwater in 1968. With
391 these values, the evolution/attenuation of a PFAS source and plume considering
392 matrix diffusion was reconstructed, potentially for the first time.

393

394 The REMChlor-MD model uses a linear isotherm to describe sorption of the
395 chemicals in both the transmissive and low-k zones of the model and cannot use
396 any other type of isotherm. PFAS sorption is the focus of considerable research,
397 and a variety of isotherms have been used to represent sorption, such as
398 Freundlich, Langmuir, Virial, and linear isotherms. Sima and Jaffe (2021) evaluated
399 the appropriateness of various isotherm types and stated that "…at low PFAS
400 concentrations, a linear K_d may be sufficient depending on soil-PFAS-solvent
401 interaction," citing four studies (Milinovic et al., 2015; Miao et al., 2017; Wei et al.,
402 2017; Li et al., 2019) as support for this statement. It should be noted that each of
403 these four studies cited in Sima and Jaffe (2021) had different conclusions about
404 which models fit their experiment data better and had different upper concentration
405 thresholds for use of a linear isotherm. More importantly, the four papers did not
406 suggest a single Freundlich model with a specific Freundlich n value that would be
407 appropriate for modeling a particular site. Therefore, for the REMChlor-MD model,
408 the use of the linear isotherm was considered an appropriate approach for this early
409 attempt to modeling PFAS in groundwater.

410

411 Using the REMChlor-MD model, the change in the PFAS Compartment Model was
412 simulated, starting from the source reaching groundwater (around 1978) to the near
413 present (2017), where the model can be adjusted to match the measured
414 compartment data, and then most importantly, into the future. With this model, key

415 questions about the site were addressed related to the migration of PFAS over the
416 past 40 years under the influence of advection, dispersion, sorption, and matrix
417 diffusion. The model was then used to indicate how far the plume might migrate in
418 future years, and better understand the effectiveness of a hypothetical complete
419 source removal project on controlling plume migration.

420

421 As such, the following model simulations for PFOS were used, and focused on
422 these key dates and subsequent REMChlor-MD evaluations:

423 • **1977**: PFOS from the source reached groundwater with a relatively
424 constant source strength, thereby creating the downgradient PFOS plume.
425 • **2017:** High-resolution site characterization was performed. REMChlor-MD
426 analyses included:
427 1) Comparison of three different REMChlor-MD models (Model A, Model
428 B, Model C) with three different representations of matrix diffusion to
429 determine which model best fit the measured site data;
430 2) Application of one best-fit model to evaluate chemical profiles with and
431 without matrix diffusion.
432 • **2020:** Hypothetical complete source removal project modeled in REMChlor-
433 MD.
434 • **2040:** Plume length forecasted at about 20 years into future from present
435 time (with and without source removal in year 2020).
436 • **2070:** Plume length forecasted at about 50 years into future from present
437 time (with and without source removal in year 2020).

438

439

440 **REMChlor-MD Input Data**

441 Site-specific characteristics were used as inputs into the REMChlor-MD models as
442 seen in Table 2. For geology, site-specific boring log data along the direction of
443 groundwater flow (Locations 3, 8, 10, 12, and 14) were used to quantify the number
444 and thickness of low-permeability layers within the plume and then entered into the
445 "heterogeneity calculator" used in the REMChlor-MD interface (Farhat et al., 2018).

446

447 For Model A, the REMChlor-MD transmissive zone was defined to include only
448 clean sands (Poorly Graded Sands (SP)). As previously described, two slug test
449 results were available for a monitoring well located in the most transmissive
450 geologic media (SP), with a geomean hydraulic conductivity of $2.4x10^{-3}$ cm/sec (6.8
451 ft/day) for this material. An evaluation of soil borings indicated the SP sands were
452 extensive enough to be continuous at the site. Therefore, the low-k geologic media
453 in Model A was defined as all fine-grained geologic soil layers with a hydraulic
454 conductivity 10 times lower than the geologic media in the REMChlor-MD
455 transmissive zone (Farhat et al., 2021). A single slug test was performed at a well
456 screened in Sands with Fines material (SM) and showed a hydraulic conductivity of
457 7.1×10^{-5} cm/sec (0.20 ft/day) or 34 times less than the more permeable SP sands.
458 Therefore, the SM soils were defined as being in the low-k compartment. The Silt
459 (ML) and Low Plasticity Clay (CL) soils were also classified as low-k units and had
460 estimated hydraulic conductivities that were 235 times and 1,821 times lower than
461 the hydraulic conductivity of the SP soils.

462

To evaluate the sensitivity of the REMChlor-MD model to the definition of what comprises low-k media, Model B assumed that the silty sand soils (SM) and clean sand (SP) were transmissive, and silt and clay (ML and CL) were low-k units. Finally, Model C was constructed to simulate plume migration with no matrix diffusion to represent conventional analytical groundwater fate and transport models with no diffusion processes.

Calibration Parameters and Best Match Metrics

The calibration effort focused on developing a REMChlor-MD model that best matched three key metrics from the 2017 site investigation:

- Concentration of PFOS at the furthest downgradient location (Location 14) (note units of μg/L per liter are used in the model interface). This is a proxy for the measured plume length at the farthest downgradient monitoring well.
- Mass discharge (kg/yr) at the source, near transect, and far transects.
- Total mass (kg) of PFOS in the near downgradient and far downgradient plumes (in both the low-k and transmissive zones).

Three model input parameters were used as calibration parameters:

- The groundwater seepage velocity, where the hydraulic conductivity and hydraulic gradient were fixed with the measured values from the site and seepage velocity was altered by changing the effective porosity;
- Longitudinal dispersivity (m); and
- The concentration in the source of the transmissive zone (ug/L).

These parameters were changed to find the best match to the three best-fit metrics. As a simplifying assumption, no transformation of precursors to form PFOS was assumed. When the high-resolution sampling was performed, most of the precursor mass in 2017 was comprised of short chain precursors that could not form PFOS (Adamson et al., 2020).

During the calibration, effective porosity of the transmissive zone was initially maintained to an approximate range of 0.02 and 0.30. The lower range represents effective porosity as described in the REMChlor-MD User's Manual (Farhat et al., 2018) when accounting for the reference to Payne et al.'s (2008) "mobile porosity" for unconsolidated hydrogeologic settings that typically falls in the 0.02 to 0.10 range. These lower effective porosities are being used more frequently in transport calculations and modeling studies. For example, the environmental consultant working at the site used an effective porosity of 0.05 for their transport calculations at this site (Consultant Report, 2017) prior to the work on this research. For the upper range, the REMChlor-MD Manual's upper range estimate of 0.30 for fine sand was used (Farhat et al., 2018).

Initially longitudinal dispersivity was constrained to within the recommended range in the REMChlor-MD manual (Farhat et al., 2018), between 3 and 21 meters. Transverse dispersivity was assumed to be 10% of the longitudinal dispersivity. Because the simulation assumed two-dimensional groundwater flow, vertical dispersity was not important to the model.

As recommended in Farhat et al. (2018), the model was run so the cell size in the x-direction was always equal or less than two times the longitudinal dispersivity for each model. Because of the low concentrations that are modeled for PFOS, a convergence tolerance of $1x10^{-5}$ ug/L was used in the model.

The initial source concentration calibration parameter reflects the PFOS concentration in the source in 1977, the year the simulation started. This concentration is assumed to be relatively constant through the life of the simulation because of the analysis previously described. To simulate a relatively steady state source concentration, the REMChlor-MD “gamma” parameter was set to zero, that when used in the Power Model, results in an unchanging source mass discharge over time until the original source mass was exhausted. In the model, the mass discharge leaving the source is about 0.44 kg/yr, and therefore the 40 kg of PFOS in the source in the model would be exhausted in about 91 years after the year the source started in 1977 or about the year 2068.

Table 2. Key REMChlor-MD Inputs for PFOS Models (2017)

Model Input	Value	Units	Source/ Notes
Years of Simulation	1977-2017	year	Historical fire training activities from 1968-1991; source began in 1977 to better match PFOS mass data in source and plume.
Transmissive Zone			
Soil Type	Poorly Graded Sand (SP)		Comprised of SP layers in Model A. Comprised of SP and SM layers in Model B.
Hydraulic Conductivity (K)	0.00239	cm/sec	Consultant Report, 2017.
Effective Porosity (Calibration parameter)	0.010 (Initial estimate) 0.11 (Model A) 0.18 (Model B) 0.28 (Model C)	(-)	Most likely value ranging between 0.02 and 0.30 from REMChlor-MD Users' Manual.
Tortuosity	0.50 (Model A and B) 0.000001 (Model C)	(-)	Default REMChlor-MD, based on K of transmissive zone media.
Hydraulic Gradient	0.0038	(-)	Consultant Report, 2017.
Primary Groundwater Flow Direction	Northeast		Towards Location 14.
Retardation Factor in T-Zone	2.9	(-)	Average R using soil-groundwater pairs of SP soil types (data from Adamson et al., 2020).
Longitudinal dispersivity (Calibration parameter)	15 (Initial Estimate) 15 (Model A) 4 (Model B) 3 (Model C)	m	Calculated in Recolor-MD using the Modified Xu and Eckstein method with plume length of 350 m.
Transverse dispersivity	1.5	m	10% of longitudinal dispersivity.
Low Permeability Zone			
Soil Type	Silt		Comprised of SM, ML, and CL layers in Model A. Comprised of ML and CL in Model B.
Hydraulic Conductivity	0.0000102	cm/sec	Consultant Report, 2017.
Porosity	0.43	(-)	Estimated using REMChlor-MD Interface based on silt.
Tortuosity	0.40	(-)	Default REMChlor-MD, based on K of low-k zone media (assumed to be silt).
Initial PFOS Source Concentration in 1977 (and subsequent years and gamma = 0 in REMChlor-MD model). (Calibration parameter)	1,342 (Initial Estimate) 1,600 (Model A) 1,400 (Model B) 1,600 (Model C)	ug/L	Calibration parameter used to match concentration of near source monitoring well. Initial estimate based on concentration of well closest to the source zone.
Source Mass at Time of Release	40	kg	Data from Adamson et al., 2020.
Retardation Factor in Low-K	2.67		Average R using soil-groundwater pairs of SM, ML and CL soil types (data from Adamson et al., 2020).
Source, Diffusion and Decay Characteristics			
Source Width	116	m	Approx. diameter of fire training area.
Molecular Diffusion Coefficient of PFOS	3.52E-6	cm^2/sec	MDEQ, 2015. For Model C, value of 3E-13 cm2/sec was used (effectively no diffusion to account for no matrix diffusion).
Mass-Flux/Remaining-Mass Term (Gamma)	0		Constant source term.

RESULTS AND DISCUSSION

Comparison of Three Different Model Calibrations

The results of the calibration exercise are shown in Table 3 and Figure 6.

Model A (With Clean Sands as Transmissive Unit): Model A required very little adjustment of initial parameter estimates, where the effective porosity was changed from 0.10 to 0.11 and the initial source concentration was increased from 1,342 to 1,600 ug/L PFOS in 1978 (Table 2). The final calibration results presented in Table 3 shows the calibrated model was able to match measured PFOS concentration at Location 14 quite closely (within 20%). The Root Mean Square Error (RMSE) between the PFOS concentrations measured in the field and the simulated concentration was 200 $ug^2 \bullet L^{-2}$, the best of all three models. Similarly, the RMSE for the mass discharge (0.049 $kg^2 \bullet year^{-2}$) comparison was significantly better than Model B and just slightly better than Model C. Most importantly, the model was able to reproduce the dominant feature of this site where significant mass is retained in low-k units as expressed in the percent distribution of PFOS mass in the low-k/ transmissive media:

- Field Data: a total of 23 kg PFOS downgradient of the source, 80% in low-k units comprised of SM, ML, and CL soils
- Model A: 18.6 kg PFOS downgradient of the source, 86% in low-k units comprised of SM, ML, and CL soils for a Low-K Mass Percent ratio of **1.08** (86%÷80%) where 1.0 is a perfect match.

Model B (Both Clean Sands and Silty Sands as Transmissive Units): An alternative conceptual model (Model B) was used for a second REMChlor-MD run where all sands (both SP and SM) were defined as transmissive media, while low permeability media included only silts and clays (ML and CL). This alternative model assumes all the transmissive media have the same hydraulic properties, so the hydraulic conductivity of the SP media was used to capture the high flow nature of this water-bearing unit. The Model B RMSE errors for both concentration and mass discharge were higher than Model A. When calibrated to the best extent possible (effective porosity of 0.25 and longitudinal dispersivity of 3 m), Model B significantly overestimated the percent of mass in the low-k compartment:

- Field Data: a total of 23 kg PFOS downgradient of the source, 21% in low-k units comprised of only ML/CL soils as a modified definition of “low-k” units;
- Model B: 31 kg PFOS downgradient of the source, 61% in low-k units comprised of only ML/CL soils for a Low-K Mass Percent ratio of **2.9** (61%÷21%) where 1.0 is a perfect match.

This evaluation of the alternate conceptual model where SM sands were lumped together with SP sands did not provide a good calibration to the percent mass in low-k units metric, and therefore supports the conceptual model (Model A) where only SP (Clean Sands) comprise the transmissive compartment.

Model C (No Matrix Diffusion): An additional calibrated No Matrix Diffusion model was attempted. An initial REMChlor-MD model run resulted in a too long groundwater plume that significantly overpredicted concentrations at Location 14, the most downgradient well. Here, in order to shorten the plume and match the field data, calibration parameters of effective porosity and longitudinal dispersivity were

applied. The Model C RMSE error for concentration (886 $ug^2 \cdot L^{-2}$) was significantly larger compared to Model A and Model B (200 and 300 $ug^2 \cdot L^{-2}$, respectively). As seen in Figure 6, the simulated concentration and mass discharge curves provide a good match to field data, but only with an extreme value of effective porosity. As a no matrix diffusion model, the Low-K Mass Percent ratio was **0.0** (i.e., Adamson et al. (2020) definitely shows significant PFAS mass present in low-K media, but this conceptual model assumes there is none). As such, this model was not considered in future simulations.

Table 3. Comparison of Calibrated Models

	Model A	***Model B***	***Model C***
Matrix Diffusion Used in Model?	YES	YES	NO
Definition of Low-k Units?	SM, ML, CL	ML, CL	None
Concentration at Loc. 14 (ng/L) (Downgradient Well)	Field Data: 1.67 Model: 1.60	Field Data: 1.67 Model: 1.54	Field Data: 1.67 Model: 1.23
Concentration RMSE (Range in Field Data: 1,342 to 1.67 ug/L)	**200**	300	886
Mass Discharge RMSE (Range in Field Data: 0.31 to 0.0053 kg/yr)	**0.049**	0.30	0.13
(Field Data Mass in Low-k Units) ÷ (Modeled Mass in Low-k units) (1.0 is perfect match)	**1.08**	2.9	0.0
Input Parameters within REMChlor-MD recommended ranges?	**YES**	**YES**	**YES***

RMSE: Root Mean Square Error. SM: Silty sand. ML: Silt. CL: Lean Clay

***BOLD:** Best performing models for a particular metric*

** However, the effective porosity of 0.28 almost exceeds the Farhat et al. (2018) recommended maximum value of 0.30 for fine sands.*

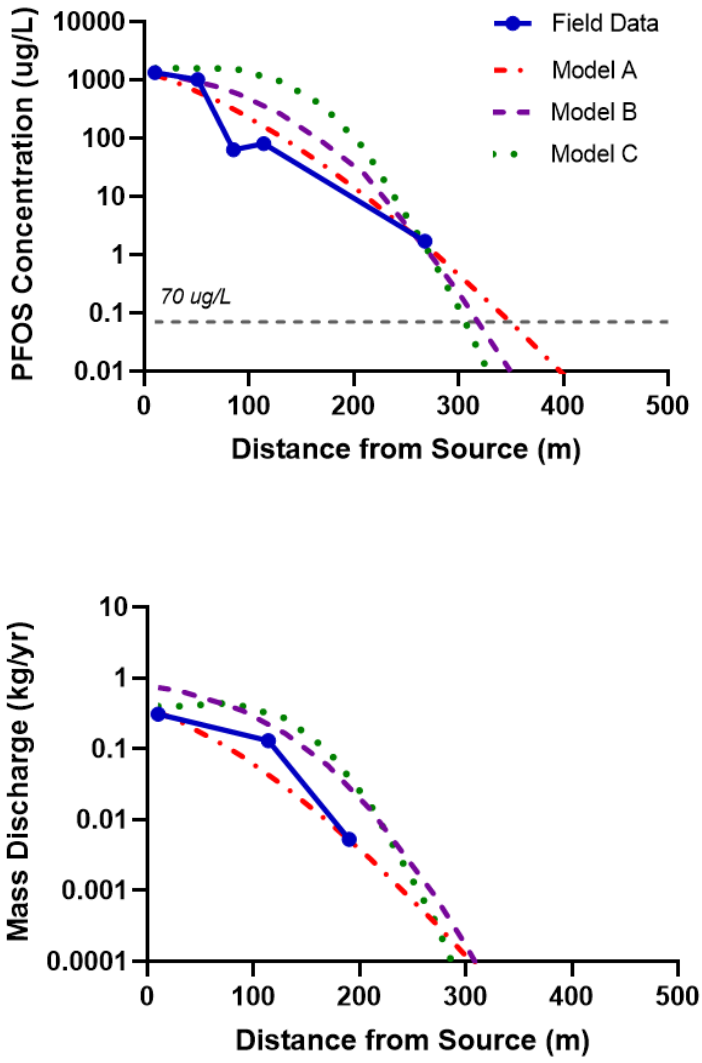

Figure 6. PFOS Concentration (Top Panel) and Mass Discharge (Bottom Panel) vs. Distance from Source (2017)

Overall, the correlation of the three key evaluation metrics (concentration, mass discharge, and total mass in the two units), indicates that REMChlor-MD **Model A** with matrix diffusion in low permeability silty sands, silts, and clays was best able to simulate the observed PFOS mass distribution from the high-resolution monitoring program for plume migration to the northeast.

Key Processes Evaluated

With the calibrated REMChlor-MD model with matrix diffusion (Model A), a hypothetical exercise to evaluate a possible maximum PFOS plume extent was conducted where the edge of the plume was assumed to be at the 0.07 µg/L (70 ppt) Preliminary Remediation Goal (USEPA, 2019). With this definition of the PFOS plume boundary, the simulated plume was on the order of 350 meters (1,150 feet) long in 2017. This is generally supported by the field observations where relatively high concentrations of PFOS were seen in the far downgradient location (1.67 µg/L in Location 14) about 270 m (890 feet) from the center of the source. However, the entire PFOS plume was not fully delineated in the field, and therefore a comparison to the full extent of the plume could not be confirmed. Overall, the base case REMChlor-MD model was considered to adequately represent the key site characteristics that impact the fate and transport of PFOS at the site and was then used to evaluate several key processes about PFOS migration.

Impact of Matrix Diffusion on Plume Migration

A second simulation of the calibrated Model A was run without matrix diffusion processes (i.e., no diffusion into low-permeability layers) by greatly reducing the diffusion coefficient by 4 orders of magnitude, while all other variables were kept constant. With this approach, the geologic conceptual model is maintained where advection is dominated by the clean sands (SP) (retained in both models) and with no change in the calibrated groundwater seepage velocity, but no matrix diffusion retention is possible for the no-matrix diffusion model.

At this site, Model A suggested the plume length to the 0.07 ug/L boundary was about 350 meters in 2017 (Figure 7). With no matrix diffusion, the simulated plume length was 910 meters, or 2.6 times longer than the with matrix diffusion case. Overall, the application of the REMChlor-MD model to this field site indicates that matrix diffusion can serve as an important attenuation process with respect to the rate of plume expansion for PFOS. A companion paper (Farhat et al., 2021) explores this matrix diffusion attention process in more detail.

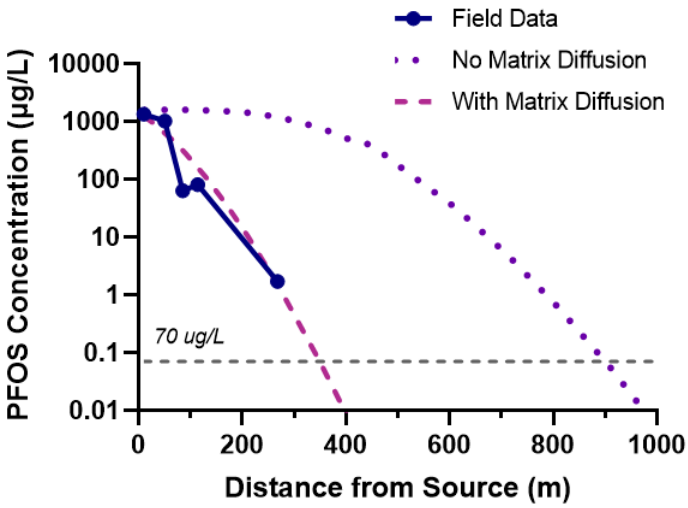

Figure 7. Simulated Plume Lengths for Model A With and Without Matrix Diffusion in 2017.

Potential Future PFOS Plume Expansion

Model A, with matrix diffusion, was then used to project the migration of the PFOS plume in the future. As a non-degrading constituent with relatively strong source, the REMChlor-MD model runs forecasts that the PFOS plume will likely continue to expand slowly, to 420 meters in the year 2040 and 500 meters in the year 2070

(Figure 8 and Table 4). These results suggest that due to the effects of dispersivity and potentially matrix diffusion, the rate of plume expansion drops significantly over time as shown in Table 4, from an average 8.8 meters per year during the first 40 years of plume expansion to only 2.7 meters per year during the period 63 to 93 years after the release.

Table 4. Modeled Plume Expansion Rates for Different Intervals, 1977 to 2070

Interval	*Start of Interval*	*End of Interval*	*Total Time (years)*	*Years in Interval (years)*	*Total Plume Length (m)*	*Plume Length Over Interval (m)*	*Plume Expansion Rate (m/year)*
1	1977	2017	40	40	350	350	8.8
2	2017	2040	63	23	420	70	3.0
3	2040	2070	93	30	500	80	2.7
Total	1977	2070	93	93	500	500	5.4

Additionally, a hypothetical source remediation project was simulated in the year 2020, where 100% of the source mass was removed. Subsequent predictions of future plume migration indicated that this hypothetical source remediation would have no impact on the plume length in the year 2040 or 2070, a finding consistent with Farhat et al. (2021) modeling results. For non-degrading plumes, source remediation has little effect on the plume expansion rate (the distance of the leading edge of the plume from the source) for the modeling scenarios shown in Figure 8. Some slight change was noticed in near source concentrations in 2040 and 2070 (dashed lines) but even these near-source areas still have elevated concentrations of PFOS after complete source remediation due to matrix diffusion.

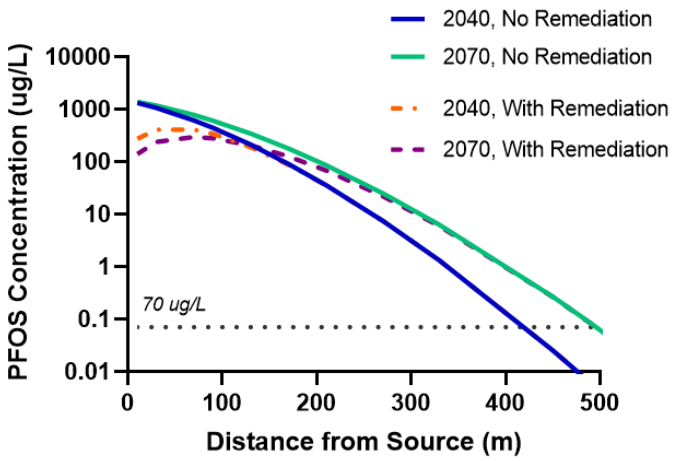

665 **Figure 8. Comparison of PFOS Concentration vs. Distance from Source in the Year**
666 **2040 and 2070, With and Without Remediation.** Note 100% of source mass removed in
667 2020.

668

669 **Model Limitations**

670 The REMChlor-MD model and the input data have several limitations that increase
671 the uncertainty in the model results. While the observed hydrogeologic setting
672 changes from the source to the downgradient portion of the plume (Figure 1), the
673 REMChlor-MD model assumes uniform values for groundwater hydraulic
674 parameters and for the model's heterogeneity parameters. In addition, REMChlor-
675 MD only allows use of a linear isotherm throughout the model domain; however,
676 while certain high-concentration portions of the modeling domain may be better
677 modeled by a Freundlich isotherm. The timing of the source term introducing PFAS
678 to the plume downgradient of the source is not likely to be much before 1968 but
679 could be earlier or later than the best estimate of 1977. A different year for the birth
680 of the plume could change some of the modeling results presented in the paper.

681

682 Additionally, the interpretations of the modeling results are based on the site
683 characterization work done at the site to date. Additional site characterization could
684 change the field data used in the calibration and provide new information about the
685 potential plume length. In addition, modeling of other PFAAs could result in different
686 modeling outcomes. Finally, the hydraulic conductivity data for the two types of
687 sandy media (fine sands and silty sands) were fixed in the model but are only based
688 on two slug tests which have a relatively large range of uncertainty. Overall, the
689 modeling results should not be considered definitive but rather indicate the general
690 style of the key fate and transport processes for PFOS at this site, processes that
691 include a significant impact from matrix diffusion.
692

693 **CONCLUSIONS**

694 The work presented herein illustrates, as with most contaminants, storage and
695 release of PFAS in low permeability zones can be an important groundwater fate
696 and transport process. When the REMChlor-MD model was applied to a well
697 characterized PFAS research site, the pre-calibration model input parameters had
698 to be adjusted only slightly when matrix diffusion was used in the model.
699

700 The modeling work suggested that the definition of what comprises transmissive vs.
701 low-k geologic media in the model is important when using REMChlor-MD to model
702 field sites. Four general soil types were logged during the site characterization
703 project: clean sands, silty sands, silts, and clays. For the purpose of modeling
704 matrix diffusion in the model, the clean sands ($K=2.4x10^{-3}$ cm/sec) was always
705 assumed to be transmissive geologic media, and silts and clays were assumed to
706 be low-k media. The fourth soil type, silty sands ($K=7.1\ x10^{-5}$ cm/sec, or 34x lower

than the clean sands) were modeled first as being low-media (Model A), then as transmissive media (Model B). Model A fit the site data much better in terms of match centerline plume concentrations, mass discharge across three transects, and the fraction of the PFOS mass in defined low-k media. These results suggest that significant matrix diffusion can occur in plumes where there are two contacting sandy soil types, and that low-k media is not confined to only silts and clays.

At this site, matrix diffusion processes appeared to have reduced the 1977 to 2017 plume length to only 350 meters compared to a no-matrix diffusion simulated plume length of 910 meters. This supports the conclusions of Farhat et al., 2021 that indicate that matrix diffusion is an important attenuation process for non-degrading groundwater chemicals such as PFOS.

With the calibrated REMChlor-MD model, future plume lengths were forecasted for the year 2070, 93 years since the groundwater source started. Using a plume boundary criteria for PFOS of 0.070 ug/L and a U.S. Environmental Protection Agency preliminary remediation goal, the PFOS plume is forecasted to grow from 350 meters in 2017 to 500 meters long in the year 2070 or 1.4 times longer than the 2017 plume length. The modeling indicates that the plume expansion rate falls significantly over time, from 8.8 meters per year during the first 40 years of plume life to only 2.7 meters per year during the interval from 63 to 93 years of plume life. This is likely due to a combination of dispersion and matrix diffusion processes (Farhat et al. 2021). Because there are no receptors that will be contacted through the year 2070 (about 50 years from now), the modeling forecasts suggested this plume could be managed in-place without the need of a pump and treat system to

control migration. However, because of the uncertainty in the modeling results, long-term monitoring would likely be required for part or all of the next 50 years. Finally, a hypothetical source remediation project in the year 2020 was forecasted to have no impact on the forecasted plume length in the year 2040 or 2070, a finding consistent with Farhat et al. (2021) modeling results. Overall, this study highlights the importance of incorporating contaminant storage and release from low-k zones into Conceptual Site Models to quantify risks and select remedies for PFAS in groundwater.

Acknowledgements. The authors would like to acknowledge the important contributions by Dr. Jennifer Field, Trever Schwichtenberg, and Alix Rodowa (Oregon State University), Anastasia Nickerson and Christopher P. Higgins (Colorado School of Mines), and Sophia Lee, Arun Gavaskar, and Dr. John Kornuc from Naval Facilities Engineering and Expeditionary Warfare Center (NAVFAC EXWC). Technical support was provided by Dr. Phil de Blanc, Kenneth Walker, Brian Strasert, Dylan Hart, Victoria Boyd, and Justin Long (GSI Environmental Inc.). We thank the base personnel for supporting the demonstration. This project was supported by Environmental Security Technology Certification Program (project ER-201633) and Naval Facilities Engineering and Expeditionary Warfare Center.

REFERENCES

3M, 2021. 3M's Commitment to PFAS Stewardship. https://www.3m.com/3M/en_US/pfas-stewardship-us/pfas-history/. Accessed 15 October 2021.

Adamson, D. and Newell, C., 2014. *Frequently asked questions about monitored natural Attenuation in Groundwater*. Environmental Security Technology Certification Program, Alexandria, Virginia. VA.

Adamson, D. T., Nickerson, A., Kulkarni, P. R., Higgins, C. P., Popovic, J., Field, J., & Kornuc, J. J., 2020. Mass-Based, Field-Scale Demonstration of PFAS Retention within AFFF-Associated Source Areas. Environmental Science & Technology, 54(24), 15768-15777.

Adamson, D.T., Kulkarni, P.K, Nickerson, A., Higgins, C.P., Field, J.A., Schwichtenberg, T., Newell, C.J., and Kornuc, J.J., 2021. Characterization of relevant site-specific PFAS fate and transport processes at multiple AFFF sites. Manuscript in review.

Anderson, R.A; Adamson, D. T.; Stroo, H. F., 2019. Partitioning of Poly- and Perfluoroalkyl Substances from Soil to Groundwater within Aqueous Film-Forming Foam Source Zones. *J. Contam. Hydrol.* 2019, *220* (2019), 59–65.

Brooks, M.C., Yarney, E. and Huang, J., 2021. Strategies for Managing Risk due to Back Diffusion. *Groundwater Monitoring & Remediation*, *41*(1), pp.76-98.

Brusseau, M.L., 2018. Assessing the potential contributions of additional retention processes to PFAS retardation in the subsurface. *Science of the Total Environment*, *613*, pp.176-185.

Brusseau, M.L., Yan, N., Van Glubt, S., Wang, Y., Chen, W., Lyu, Y., Dungan, B., Carroll, K.C. and Holguin, F.O., 2019. Comprehensive retention model for PFAS transport in subsurface systems. *Water research*, *148*, pp.41-50.Chapman, S. W., & Parker, B. L. (2005). Plume persistence due to aquitard back diffusion following dense nonaqueous phase liquid source removal or isolation. *Water Resources Research*, *41*(12), 1–16. https://doi.org/10.1029/2005WR004224

Chapman, S. W., & Parker, B. L., 2005. Plume persistence due to aquitard back diffusion following dense nonaqueous phase liquid source removal or isolation. Water Resources Research, 41(12), 1–16. https://doi.org/10.1029/2005WR004224

Chapman, S.W., Parker, B.L., Sale, T.C., Doner, L.A., 2012. Testing high resolution numerical models for analysis of contaminant storage and release from low permeability zones. Journal of Contaminant Hydrology, 136, pp. 106-116. DOI: 10.1016/j.jconhyd.2012.04.006

Consultant Report, 2017. Technical Memorandum: Perfluorinated Compounds (PFC) Assessment Petroleum at Petroleum Contaminated Area 15 Fire Fighter Training Facility NAS Jacksonville. Prepared by: Solutions IES. August 2017.

Costanza, J., Arshadi, M., Abriola, L. M., & Pennell, K. D., 2019. Accumulation of PFOA and PFOS at the Air-Water Interface. *Environmental Science and Technology Letters*, *6*(8), 487–491. https://doi.org/10.1021/acs.estlett.9b00355

Falta, R. W., Suresh Rao, P., & Basu, N., 2005. Assessing the impacts of partial mass depletion in DNAPL source zones: I. Analytical modeling of source

796 strength functions and plume response. *Journal of Contaminant Hydrology*,
797 *78*(4), 259–280. https://doi.org/10.1016/j.jconhyd.2005.05.010

798 Falta, R. W., & Wang, W., 2017. A semi-analytical method for simulating matrix
799 diffusion in numerical transport models. *Journal of Contaminant Hydrology*, *197*,
800 39–49. https://doi.org/10.1016/j.jconhyd.2016.12.007

801 Falta, R. W., Farhat, S. K., Newell, C. J., & Lynch, K., 2018. A Practical Approach
802 for Modeling Matrix Diffusion Effects in REMChlor. Clemson University Clemson
803 United States.

804 Farhat, S. K., Newell, C. J., Seyedabbasi, M. A., McDade, J. M., Mahler, N. T., Sale,
805 T. C., Dandy, D. S., & Wahlberg, J. J., 2012. Matrix Diffusion Toolkit.
806 https://www.serdp-estcp.org/Tools-and-Training/Environmental-
807 Restoration/Groundwater-Plume-Treatment/Matrix-Diffusion-Tool-Kit

808 Farhat, S.K., Newell, C.J., Falta, R.W., and Lynch, K., 2018. *REMChlor-MD User's*
809 *Manual.* Developed for the Environmental Security Technology Certification
810 Program. ESTCP project ER-201426, Alexandria, VA.

811 Farhat, S.K., Adamson, D.T., Gavaskar, A.R., Lee, S.A., Falta, R.W., and. Newell,
812 C.J., 2020. "*Vertical Discretization Impact in Numerical Modeling of Matrix*
813 *Diffusion in Contaminated Groundwater."* Groundwater Monitoring and
814 Remediation 40 (2): 52–64. https://doi.org/10.1111/gwmr.12373.

815 Farhat, S.K., C.J. Newell, Lee S.A., Looney B.B., and Falta R.W., 2021*. Impact of*
816 *Matrix Diffusion on the Migration of Groundwater Plumes for Non-Degradable*
817 *Compounds such as Perfluoroalkyl Acids (PFAAs).* Submitted to Journal of
818 Contaminant Hydrogeology, Oct. 2021.

819 Foster, S. S. D., 1975. *The Chalk groundwater tritium anomaly—a possible*
820 *explanation*. Journal of Hydrology, 25(1-2), 159-165.

821 Gillham, R. W., Sudicky, E. A., Cherry, J. A., & Frind, E. O., 1984. An Advection-
822 Diffusion Concept for Solute Transport in Heterogeneous Unconsolidated
823 Geological Deposits. *Water Resources Research*, *20*(3), 369–378.
824 https://doi.org/10.1029/WR020i003p00369

825 Golden Software, 2019. Voxler Power Forward Into 3D Visualization.
826 https://www.goldensoftware.com/products/voxler/features Accessed Dec. 22,
827 2020.

828 Grandjean, P., Clapp, R., 2015. *Perfluorinated alkyl substances: emerging insights*
829 *into health risks*. New Solutions. A Journal of Environmental and Occupational
830 Health Policy 25 (2), 147–163. https://doi.org/10.1177/1048291115590506.

831 Guelfo, J. L.; Higgins, C. P., 2013. Subsurface transport potential of perfluoroalkyl
832 acids at aqueous film-forming foam (AFFF)-impacted sites. *Environ. Sci.*
833 *Technol.* 2013, *47*(9), 4164-4171

834 Guo, B., Zeng, J. , and Brusseau, M.L., 2020. "A Mathematical Model for the
835 Release, Transport, and Retention of Per- and Polyfluoroalkyl Substances
836 (PFAS) in the Vadose Zone." Water Resources Research 56 (2):
837 e2019WR026667. https://doi.org/10.1029/2019WR026667.

838 Higgins, C. P.; Luthy, R. G. 2007. Modeling sorption of anionic surfactants onto
839 sediment materials: an a priori approach for perfluoroalkyl surfactants and linear
840 alkylbenzene sulfonates. *Environ. Sci. Technol.* 2007, *41*(9), 3254-3261.

Kulkarni, P.R., Godwin, W.R., Long, J.A., Newell, R.C., Newell, C.J., 2020. How much Heterogeneity: Flow vs. Area from a Big Data Perspective. Remediation Journal. 30. 15-23.

Li, Y., Oliver, D. P., & Kookana, R. S., 2018. A critical analysis of published data to discern the role of soil and sediment properties in determining sorption of per and polyfluoroalkyl substances (PFASs). *Science of the Total Environment*, *628–629*, 110–120. https://doi.org/10.1016/j.scitotenv.2018.01.167

Li, F., Fang, X., Zhou, Z., Liao, X., Zou, J., Yuan, B., & Sun, W., 2019. Adsorption of perfluorinated acids onto soils: Kinetics, isotherms, and influences of soil properties. *Science of The Total Environment*, *649*, 504–514. https://doi.org/https://doi.org/10.1016/j.scitotenv.2018.08.209

MDEQ, 2015. Chemical Update Worksheet, Perfluorooctane Sulfonic Acid. Michigan Department of Environmental Quality Remediation and Redevelopment Division. https://www.michigan.gov/documents/deq/deq-rrd-chem-PerfluorooctaneSulfonicAcidDatasheet_527676_7.pdf

Miao, Y., Guo, X., Dan Peng, Fan, T., & Yang, C.,2017. Rates and equilibria of perfluorooctanoate (PFOA) sorption on soils from different regions of China. *Ecotoxicology and Environmental Safety*, *139*, 102–108. https://doi.org/10.1016/j.ecoenv.2017.01.022

Milinovic, J., Lacorte, S., Vidal, M., & Rigol, A., 2015. Sorption behaviour of perfluoroalkyl substances in soils. *Science of The Total Environment*, *511*, 63–71. https://doi.org/https://doi.org/10.1016/j.scitotenv.2014.12.017

Muskus, N., & Falta, R. W., 2018. Semi-analytical method for matrix diffusion in heterogeneous and fractured systems with parent-daughter reactions. *Journal of Contaminant Hydrology*, *218*, 94–109. https://doi.org/10.1016/j.jconhyd.2018.10.002

Newell, C. J., & Adamson, D. T., 2005. Planning-level source decay models to evaluate impact of source depletion on remediation time frame. *Remediation*, *15*(4), 27–47. https://doi.org/10.1002/rem.20058

Newell, C. J., Kueper, B. H., Wilson, J. T., & Johnson, P. C., 2014. Natural Attenuation Of Chlorinated Solvent Source Zones. In B. H. Kueper, H. F. Stroo, C. M. Vogel, & C. H. Ward (Eds.), *Chlorinated Solvent Source Zone Remediation* (pp. 459–508). Springer New York. https://doi.org/10.1007/978-1-4614-6922-3_13

Newell, C. J., Adamson, D. T., Kulkarni, P. R., Nzeribe, B. N., & Stroo, H., 2020. Comparing PFAS to other groundwater contaminants: Implications for remediation. Remediation Journal, 30(3), 7-26.

Newell, C.J., Adamson D.T., Kulkarni P.R., Nzeribe, B.N., Connor, J.A., Popovic, J., and Stroo, H.F., 2021a. Monitored Natural Attenuation To Manage PFAS Impacts To Groundwater: Scientific Basis. Accepted Groundwater Monitoring and Remediation.

Newell, C.J., Adamson D.T., Kulkarni P.R., Nzeribe, B.N., Connor, J.A., Popovic, J., and Stroo, H.F., 2021b. Monitored Natural Attenuation To Manage PFAS Impacts To Groundwater: Potential Guidelines. Remediation Journal. https://doi.org/https://doi.org/10.1002/rem.21697

886 Nickerson, A., Rodowa, A. E., Adamson, D. T., Field, J. A., Kulkarni, P. R., Kornuc,
887 J. J., & Higgins, C. P., 2020. Spatial trends of anionic, zwitterionic, and cationic
888 PFASs at an AFFF-impacted site. Environmental Science & Technology, 55(1),
889 313-323.

890 National Research Council., 2005. *Contaminants in the Subsurface: Source Zone*
891 *Assessment and Remediation*. National Research Council.
892 https://doi.org/10.17226/11146

893 National Research Council., 2013. Alternatives for Managing the Nation's Complex
894 Contaminated Groundwater Sites. In *Alternatives for Managing the Nation's*
895 *Complex Contaminated Groundwater Sites*. National Research Council.
896 https://doi.org/10.17226/14668

897 Office of Solid Waste and Emergency Response., 2019. Assessing And
898 Remediating Low Permeability Geologic Materials Contaminated By Petroleum
899 Hydrocarbons From Leaking Underground Storage Tanks: A Literature Review
900 [Technical Report]. U.S. Environmental Protection Agency. Retrieved from
901 https://www.epa.gov/sites/production/files/2020-01/documents/final-low-
902 permeability-12-2-19.pdf

903 Payne, F., Quinnan, J., & Potter, S., 2008. Remediation hydraulics. Boca Raton, FL:
904 CRC Press.

905 Rao, P.S.C., Jawitz, J.W., Enfield, C.G., Falta, R., Annabel, M.D., Wood, A.L., 2001.
906 Technology integration for contaminated site remediation: cleanup goals and
907 performance metrics. Ground Water Quality. Sheffield, UK, pp. 410–412.

908 Sale, T., Newell, C., Stroo, H., Hinchee, R., & Johnson, P., 2008. *Frequently asked*
909 *questions regarding management of chlorinated solvents in soils and*
910 *groundwater*. Environmental Security Technology Certification Program
911 (ESTCP).

912 Sale, T., Parker, B. L., Newell, C. J., & Devlin, J. F., 2013. Management of
913 Contaminants Stored in Low Permeability Zones-A State of the Science Review.

914 Sima, M. W., & Jaffé, P. R., 2021. A critical review of modeling Poly- and
915 Perfluoroalkyl Substances (PFAS) in the soil-water environment. *The Science*
916 *of the Total Environment*, *757*, 143793.
917 https://doi.org/10.1016/j.scitotenv.2020.143793

918 Silva, J. A. K., Šimůnek, J., & McCray, J. E., 2020. A Modified HYDRUS Model for
919 Simulating PFAS Transport in the Vadose Zone. *Water*, *12*(10).
920 https://doi.org/10.3390/w12102758

921 Simon, J. A., Abrams, S., Bradburne, T., Bryant, D., Burns, M., Cassidy, D., ... &
922 Wice, R., 2019. PFAS Experts Symposium: Statements on regulatory policy,
923 chemistry and analytics, toxicology, transport/fate, and remediation for per-and
924 polyfluoroalkyl substances (PFAS) contamination issues. Remediation Journal,
925 29(4), 31-48.

926 Sudicky, E. A., & Frind, E. O., 1982. Contaminant transport in fractured porous
927 media: Analytical solutions for a system of parallel fractures. *Water Resources*
928 *Research*, *18*(6), 1634–1642. https://doi.org/10.1029/WR018i006p01634

929 USDA, 2012. Field Book for Describing and Sampling Soils. National Soil Survey
930 Center Natural Resources Conservation Service U.S. Department of Agriculture.
931 September 2012.

USEPA., 2019. *Assessing and Remediating Low Permeability Geologic Materials Contaminated by Petroleum Hydrocarbons from Leaking Underground Storage Tanks.* Office of Solid Waste and Emergency Response Office of Underground Storage Tanks Washington, D.C. Dec. 2019. https://www.epa.gov/sites/default/files/2020-01/documents/final-low-permeability-12-2-19.pdf Accessed Oct. 14, 2021.

U.S. Environmental Protection Agency (USEPA). 2019. Draft interim recommendations to address groundwater contaminated with perfluorooctanoic acid and perfluorooctane sulfonate. Washington, DC: U.S. Environmental Protection Agency (USEPA).

United States Geologic Survey (USGS), 2000. Fate and Transport Modeling of Selected Chlorinated Organic Compounds at Operable Unit 3, U.S. Naval Air Station, Jacksonville, Florida. Open-File Report 00-255.

Vinsome, P.K.W., Westerveld, J., 1980. A simple method for predicting cap and base rock heat losses in thermal reservoir simulators. J. Can. Pet. Technol. 87–90 July– September.

Wei, C., Song, X., Wang, Q., & Hu, Z., 2017. Sorption kinetics, isotherms and mechanisms of PFOS on soils with different physicochemical properties. *Ecotoxicology and Environmental Safety*, *142*, 40–50. https://doi.org/https://doi.org/10.1016/j.ecoenv.2017.03.040

You, X., Liu, S., Dai, C., Guo, Y., Zhong, G., & Duan, Y., 2020. Contaminant occurrence and migration between high- and low-permeability zones in groundwater systems: A review. *Science of The Total Environment*, *743*, 140703. https://doi.org/https://doi.org/10.1016/j.scitotenv.2020.140703